Available online at www.sciencedirect.com

SciVerse ScienceDirect

Ceramics International 38 (2012) 3191–3196

CERAMICS INTERNATIONAL

www.elsevier.com/locate/ceramint

Effect of variation of NiO on properties of NiO/GDC (gadolinium doped ceria) nano-composites

A.U. Chavan [a], L.D. Jadhav [b,*], A.P. Jamale [a], S.P. Patil [a], C.H. Bhosale [a], S.R. Bharadwaj [c], P.S. Patil [a]

[a] Department of Physics, Shivaji University, Kolhapur 416 004, India
[b] Department of Physics, Rajaram College, Kolhapur 416 004, India
[c] Applied Chemistry Division, BARC, Trombay, Mumbai 400 085, India

Received 17 November 2011; accepted 12 December 2011
Available online 19 December 2011

Abstract

In the present work, systematic study of series of NiO_x $GDC_{(1-x)}$ where $x = 0.1–0.6$; has been reported for the first time. For the synthesis of homogeneous NiO–GDC nanocomposite powders, the nano-powders of NiO and $Ce_{0.9}Gd_{0.1}O_{1.95}$ (GDC10) synthesized by solution combustion synthesis were mixed in mol % proportion. NiO–GDC nanocomposite can be reduced in situ to form Ni–GDC cermet anode. Hence the Ni–GDC cermet anode combines the catalytic activity and high electronic conduction property of Ni and ionic conductivity of GDC. Nano-crystalline constituents in the NiO–GDC nano composite are believed to give better anodic performance than microcrystalline constituents. Hence the efficient study of the atomistic structure and the accurate characterization of the structural parameters, such as crystallite size and internal strains, are of considerable interest. Therefore the NiO_x–$GDC10_{1-x}$ nanocomposite powders were characterized by XRD and FTIR spectroscopy. Further these powders were pelletized, sintered and characterized by FE-SEM and d.c. conductivity.

Keywords: Combustion synthesis; Nano-composite; Strain; FESEM; Density

1. Introduction

Nanostructured materials have attracted great interest for many different applications, due to their unusual or enhanced properties compared with bulk materials. The nano structured solid conductors, known as ''nanoionics'', with enhanced ionic conductivity have recently become one of the newest field of research since they can be used in advanced energy conversion and storage applications, such as solid oxide fuel cell (SOFC). To keep pace with this nanoionics, development of suitable nano-electrodes has become equally imperative.

Composite electrodes are basically physical mixtures consisting of two or more solid phases that possess mixed conductivity, i.e. ionic and electronic conductivity. An electrical composite consisting of ionic and electronic phases are of great importance [1–4] in batteries, gas sensors, membranes and in SOFC, particularly, as anode material. Ionic-, electronic nano-composite not only increase the length of triple phase boundary but also provides thermal expansion match with electrolyte, improves electrode catalytic reactions and thereby fuel cell performance. This kind of nano-composites usually shows conductivity significantly higher than in both of the constituent phases. Hence in NiO–GDC nanocomposite both NiO and GDC in composite are stable over a wide range of temperature. Moreover, NiO acts as good catalyst for oxygen activation [5], and provides good electrical conductivity while GDC10 mainly acts as matrix to support the catalyst and prohibit the Ni from agglomeration under operating conditions [6]. A nano-composite NiO–$Ce_{0.9}Gd_{0.1}O_{1.95}$ (GDC10) can be reduced in situ during the first operation of SOFC [7,8]. Although Ni–GDC (or CeO_2) composite cermet have been widely used as an anode material, very little has been reported regarding the systematic study of complete series of NiO_x $GDC_{(1-x)}$ where $x = 0.1–0.6$.

Ni–GDC composite anode, which is an ideal anode material to match with GDC electrolyte operating in the low-temperature range, has been paid more attention in recent

* Corresponding author. Fax: +91 02312691533; mobile: +91 9890694409.
E-mail addresses: chavan_au@yahoo.co.in (A.U. Chavan), ldjadhav.phy@gmail.com (L.D. Jadhav).

0272-8842/$36.00
doi:10.1016/j.ceramint.2011.12.023

years [9]. However, it has never been reported the mol % variation of NiO and GDC in NiO–GDC nanocomposite. Since the anode performance is dependent strongly on its composition, fabrication process and the resulting microstructure, it is of great interest to investigate the proper composition of the precursor anode material, i.e. NiO–GDC. The objective of this paper is to present the systematic study of NiO–GDC. Hence in present work, nano-composites were prepared by a mechanical mixing method, where NiO and $G_{0.1}C_{0.9}O_{1.95}$ (hereafter termed as GDC) powders were separately prepared by solution combustion synthesis (SCS) as the solution combustion is cost effective method for the synthesis of nano-size materials for different advanced applications, including catalysts, fuel cells, and biotechnology. It gives homogeneous, crystalline and un-agglomerated multi-component oxide ceramic powders. The NiO–GDC nano-composites were characterized by various physico-chemical techniques.

2. Experimental

The synthesis of GDC has been reported in detail in [10]. Metal nitrates $Ce(NO_3)_3{\cdot}6H_2O$ and $Gd(NO_3)_3{\cdot}6H_2O$ were used as oxidants and $C_2H_5NO_2$ as a fuel and their stoichiometric amounts were dissolved in deionized water. With the help of burette the fuel was added drop by drop while stirring at room temperature to form homogeneous solution of metal nitrates and fuel. This solution was heated on a hot plate for the removal of moisture and to form gel. Further this gel was allowed to combust in muffle furnace preheated at 325 °C. The spontaneous ignition occurred leads to pale-yellow ash [11]. The resultant ash was then collected and calcined in air at 600 °C for 2 h to remove any carbon based residues remained in the oxide powder. Similar procedure was repeated to form NiO wherein $Ni(NO_3)_2{\cdot}6H_2O$ was used as metal nitrate and glycine as fuel and formed ash was calcined at 500 °C for 2 h. Hence the morphology of the particles in ceramic materials is a consequence of the preparation method, and the combustion method favors obtaining porous nanoparticles, because the reactions produce homogeneous materials composed of small and uniform particles. The nano powders of GDC and NiO were characterized by XRD and FTIR.

The nano-composites NiO_x–$GDC_{(1-x)}$ where $x = 0.1$, 0.2, 0.3, 0.4, 0.5, 0.6 (in mol %) were formed by mixing the nano powders of NiO and GDC in agate mortar for 3 h. After formation of homogeneous mixture these nanocomposite powders were pelletized using hydraulic press and firstly pre-sintered at 900 °C for 2 h and then final sintered at 1000 °C for 8 h with heating rate of 1 °C/min. These six nanocomposite samples were named as N1G1, N2G1, N3G1, N4G1, N5G1, N6G1 respectively for $x = 0.1$, 0.2, 0.3, 0.4, 0.5, 0.6 in NiO_x–$GDC_{(1-x)}$.

Structural studies of these samples were carried out by XRD (Phillips-3710 powder X-ray diffractometer) in the 2θ range 10–90° using $CuK_{\alpha 1}$ radiation ($\lambda = 1.54056$ Å). The XRD patterns were compared with standard JCPDS files of NiO (78-0643; cubic NiO) and GDC10 (75-0161). The morphology of the composites was studied using field emission scanning electron microscope (FE-SEM). FTIR absorption behavior of these samples was obtained using Perkin Elmer, FTIR Spectrum One; with scanning range 4000–400 cm^{-1}. The conventional Archimedes method was used to measure the density of these samples. The d.c. electrical conductivity measurements were carried out by two-probe method with in temperature range of 35–700 °C. The silver current collectors were used on NiO–GDC surface having 1 mm thickness and 2 cm diameter.

3. Results and discussion

3.1. X-ray diffraction (XRD)

The XRD patterns of as prepared GDC10 and NiO powders and NiO_x–GDC_{1-x} (where $x = 0.1$–0.6) nano-composites are shown in Fig. 1. All the diffraction patterns show broad reflection peaks indicating nano powders and nano-composites. All XRD patterns were indexed using JCPDS file no. 78-0643 and 75-0161, respectively, for NiO and GDC10 phase. The XRD pattern of as prepared GDC10 shows fluorite structure with no Gd_2O_3 phase thus forming an oxide solid solution. However, the as prepared NiO shows reflection peaks due to NiO and Ni. It is seen that only about 15% Ni is present in the as prepared NiO powder, which is completely oxidized to NiO upon calcination at 600 °C [12].

The XRD patterns of the composites (Fig. 1c–h) show fluorite GDC and cubic NiO, no intermediate phase is observed, which indicates no solid solution between GDC and NiO. The reflection peaks due to NiO are very less intense, which grow with further increase in NiO content [13]. The NiO reflection corresponding to $2\theta = 75.4°$ is almost absent up to 30 mol % NiO and appear for higher NiO content. The lattice parameters of GDC and NiO phase were computed for all the nano-composites and as expected lattice parameters were independent of x and are 5.418 ± 0.005 Å and 4.176 ± 0.0002 Å, respectively for GDC10 and NiO. Very often, crystallite size is

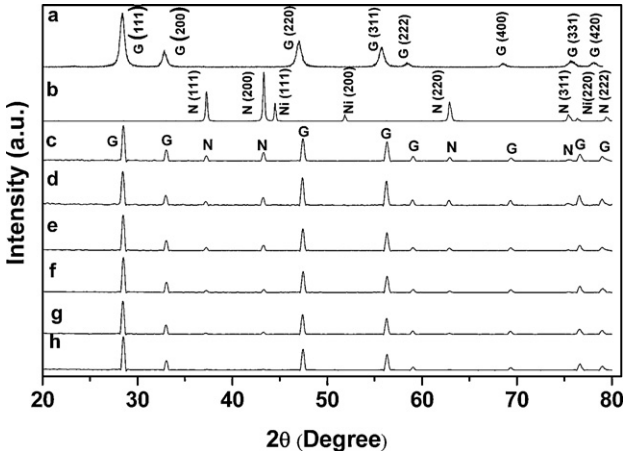

Fig. 1. XRD patterns of (a) as synthesized GDC, (b) as synthesized NiO and sintered, (c) N6G1, (d) N5G1, (e) N4G1, (f) N3G1, (g) N2G1, (h) N1G1.

obtained using Debye–Scherrer's formula,

$$D = \frac{0.9\,\lambda}{\beta \cos\theta} \quad (1)$$

where D is crystallite size, λ is the wavelength of source, β is the full width at half maximum (FWHM) of the peak and θ is the Bragg angle. Crystallite size of GDC and NiO phase in nano-composites, irrespective of NiO content, has remained same. This is obvious as nano composites are obtained by mechanical mixing of separately prepared GDC and NiO nano-powders and not from NiO–GDC nanocomposite powders. The crystallite size of GDC is 20–26 nm and that of NiO is 20–25 nm.

Nevertheless, a peak broadening is a combined effect of crystallite size and microstrain, if any, as given by Williamson and Hall equation [14],

$$\beta_t = \left[\frac{0.9\,\lambda}{D\cos\theta}\right] + [4\varepsilon \tan\theta] \quad (2)$$

$$\beta_t = \beta - \beta_0$$

where β_t is the total broadening, β_0 is the instrumental broadening, ε is the micro-strain and other notations as described for Eq. (1). The slope of the graph of $\beta_t \cos\theta$ vs $\sin\theta$ gives strain and its intercept on Y-axis gives the crystallite size. Williamson and Hall graphs were plotted for both GDC and NiO phases in nano-composites (not shown here) and then effective crystallite size and microstrain were calculated. The effective crystallite size is in the range 40–50 nm and 30–58 nm for GDC and NiO, respectively. A variation in crystallite size using Scherrer equation and Williamson and Hall equation are in close agreement.

A micro strain is caused by processing parameters and most preferably by the difference in the thermal expansion coefficients. It is reported that microstrain is caused by the defects in the material. Variation in micro-strain in GDC and NiO phase with 'x' is shown in Fig. 2a and b. The strain in NiO is tensile and is compressive in GDC. NiO–GDC nanocomposite has two different phases; GDC being ionic and NiO being electronic. Despite this, strain in the nanocomposite is very small, which is assigned to relatively close matching of thermal expansion coefficients of GDC ($12 \times 10^{-6}\,K^{-1}$) and NiO ($14 \times 10^{-6}\,K^{-1}$).

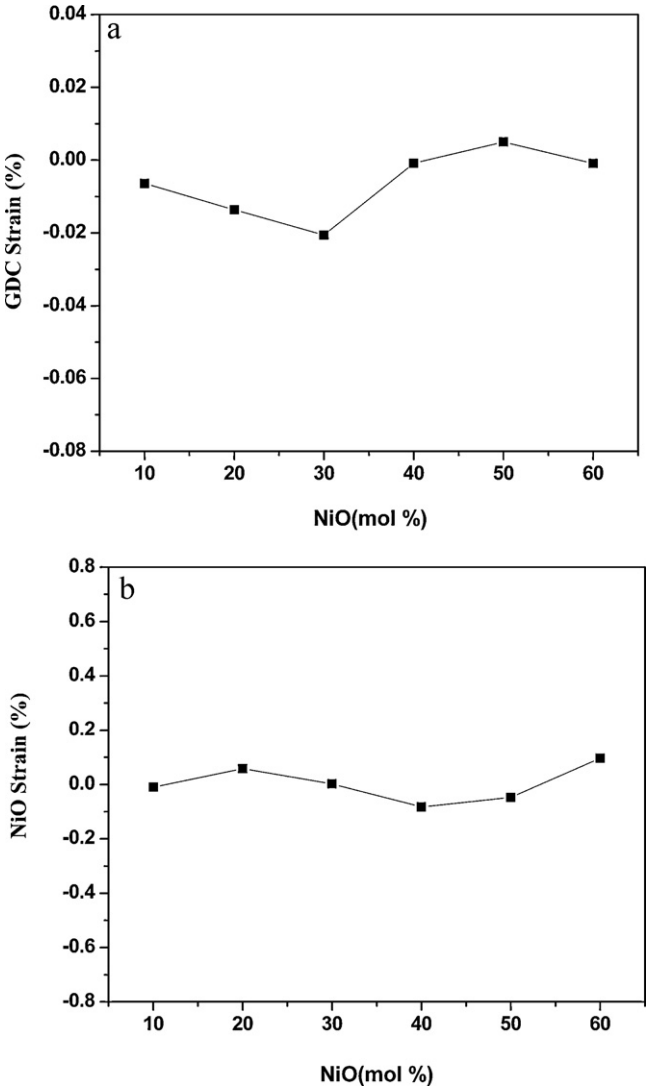

Fig. 2. (a) Variation of GDC strain with NiO Content. (b) Variation of NiO strain with NiO Content.

3.2. FTIR

Fig. 3 shows the typical FTIR spectra for the GDC, NiO and N4G1 nano-composite as well as that of pure glycine. IR spectra of glycine (Fig. 3A) shows many absorption bands in the region 1000–1750 cm^{-1}, which are attributed to the C–N, COO, C–C stretching vibrations [15]. These major absorption bands are absent in the IR spectra of GDC and NiO. Hence it is confirmed that there is no impurity due to glycine in the combustion synthesized products. The major absorption band at 3393 cm^{-1} and 3397 cm^{-1} observed respectively for GDC and NiO (Fig. 3B and C) is due to O–H stretching vibrations while the bands at 2920 cm^{-1} and 2850 cm^{-1} are attributed to the C–H vibrations. Also a weak absorption band is observed at 1019 cm^{-1} and is assigned to the C–N stretching vibrations. A broad M–O type of band at 564 cm^{-1} is assigned to nano-crystalline Ce–O while those in the region 550–700 cm^{-1} are assigned to NiO stretching vibrations [16,17].

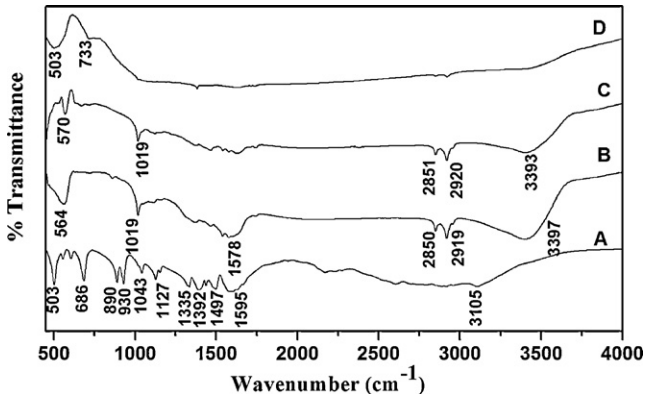

Fig. 3. FTIR spectra of (A) glycine, (B) GDC, (C) NiO and (D) one of the nanocomposite, i.e. N4G1.

Table 1
Variation of density and activation energies (E_a) with different mol % of NiO.

Sample name	Density			Activation energy (eV) 500–700 °C
	X-ray density	Actual density	% Density	
N1G1	7.23	6.80	94.05	0.8
N2G1	7.20	6.74	93.48	0.76
N3G1	7.18	6.63	92.32	0.58
N4G1	7.15	6.53	91.30	0.55
N5G1	7.12	6.32	88.82	0.56
N6G1	7.08	6.15	86.84	0.50

Besides, a band at 1578 cm^{-1} is observed for GDC and is due to –COO– asymmetrical vibrations. A weak band near 1637 cm^{-1}, observed for NiO, is assigned to the H–O–H bending vibration mode, which is due to the absorption of water in air when FTIR sample disks were prepared in an open air.

In Fig. 3D the spectrum for one of the nano-composite samples (N4G1) is shown. The broad absorption bands in the

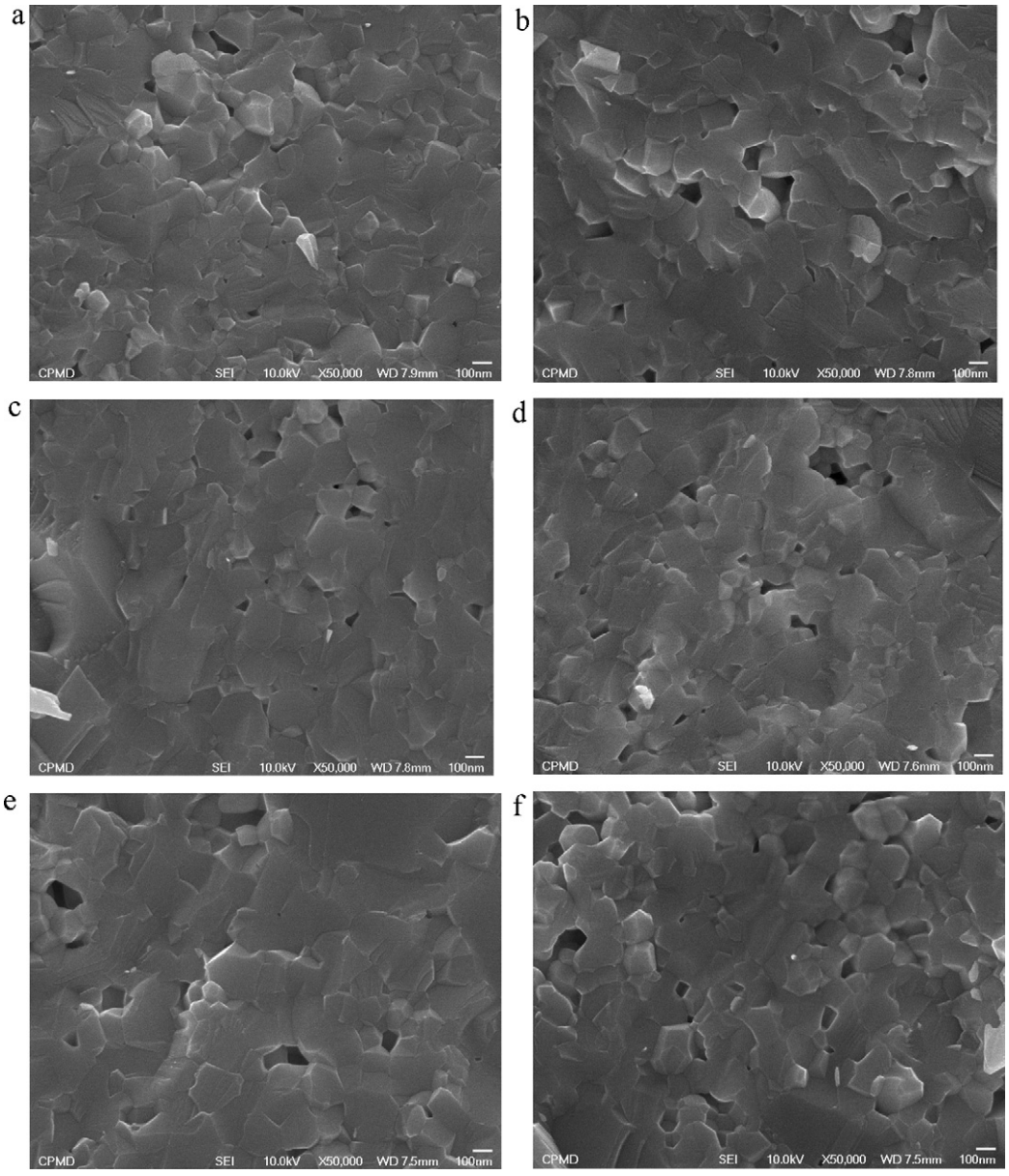

Fig. 4. FESEM images of (a) N1G1, (b) N2G1, (c) N3G1, (d) N4G1, (e) N5G1 and (f) N6G1.

region 500 and 750 cm^{-1} can be assigned to the NiO and GDC stretching vibrations. The intensity of absorption bands due to O–H, C–H and C–N vibrations is very negligible. Thus nanocomposites are pure.

3.3. Density measurements and microstructure

X-ray density of individual phases, here GDC and NiO was calculated by using the formula,

$$\rho_x = \frac{4M}{Na^3} \quad (3)$$

where M is the molecular weight, a is the lattice parameter, and N is the Avogadro's number.

Similarly X-ray density of nanocomposite samples was calculated by using the formula,

$$\rho_{\text{composite}} = \frac{M_1 + M_2}{V_1 + V_2} \quad (4)$$

where $M_1 = x \times$ (molecular weight of GDC); $M_2 = (1-x) \times$ (molecular weight of NiO); $V_1 = M_1/\rho_{x1}$ and $V_2 = M_2/\rho_{x2}$; ρ_{x1} and ρ_{x2} are X-ray densities of GDC and NiO, respectively.

The X-ray density of the all nanocomposite samples calculated using Eq. (3) is tabulated in Table 1. While experimentally density was calculated by Archimedes principle, more appropriate technique for the determination of density of porous material, and values are tabulated in Table 1. It is seen from table that both X-ray and actual density decrease with an increase in NiO content. The results were used to estimate percentage porosity. The porous microstructure can be seen in Fig. 4. Fig. 4 shows fracture FESEM of all nanocomposites and shows well-connected, non-spherical grains with sharp edges. The two phases (Ni and GDC) are uniformly distributed and well connected, which is desirable for anodic reactions and electronic conduction. In the present work, nanocomposites were sintered at 1000 °C in air atmosphere. So densification occurred by grain growth process. But NiO content drags the rate of grain growth in GDC in analogy with the results discussed in [18]. Hence porosity increases with NiO content.

3.4. D.C. conductivity measurement

The cermet conductivity occurs through two mechanisms: ionic (through the GDC phase) and electronic (through the metallic nickel phase) [19]. The d.c. electrical conductivity of the pellets for all six compositions was measured by two-probe method in the temperature range 200–700 °C in air. The d.c. conductivity fits linearly into the Arrhenius relation:

$$\sigma = \frac{A}{T}\exp\frac{E_a}{kT} \quad (5)$$

The conductivity of all nano-composite at 600 °C, a probable operating temperature of a device, is shown in Fig. 5. It shows S type behavior with increase in conductivity up to 40 mol % NiO. For NiO concentrations below 40 mol %, the conductivity is predominantly ionic. Above 40 mol %, it is predominantly electronic (typical of metals). The conductivity almost saturates above 40 mol % NiO. This shows percolation limit. As the requirement of the anode of SOFC is that, it should be electronically as well as ionically conducting. In the present study the electrical conductivity of the NiO–GDC nanocomposite attains its maximum at NiO percolation estimated to be at approximately 40 mol % [20].

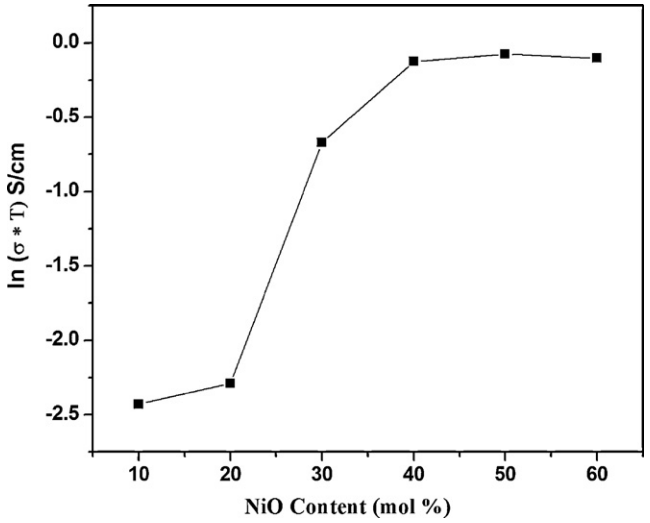

Fig. 5. Variation of electrical conductivity with NiO content at 600 °C.

The activation energy E_a was estimated using d.c. conductivity measured between 500 and 700 °C and values are tabulated in Table 1. It is seen from table that activation energy for 10 mol % NiO is 0.8 eV, which is decreased to 0.55 eV for 40 mol % NiO showing percolative behavior in NiO–GDC nano-composite. The activation energy decreased steadily for further additions of NiO.

For low NiO content, NiO is distinctly distributed throughout the composite and NiO, GDC connectivity is poor. Hence ionic conductivity is dominated over the electronic. But the activation energy less than 1 eV implies that NiO contributed to the electric conductivity. For further NiO additions, NiO and GDC are homogeneously distributed thereby forming three dimensional connectivity. Now as electronic content is increased, both ionic and electronic conductivity contributes to total conductivity. It is also expected that NiO–GDC contacts would increase leading conduction path along the interface between NiO and GDC. This needs further insights into microstructure and a.c. impedance, which is in progress.

4. Conclusions

We have successfully studied the structural, electrical conductivity, microstructure and mechanical properties of the NiO–GDC nano-composites with respect to the NiO mol %. The average crystallite size variations determined using Sherrer's formula is in agreement with those obtained from the Hall equation. For all nanocomposite samples the strain calculations using Hall equation revealed the presence of

tensile strain in NiO and compressive strain in GDC phase. The presence of vibrational bands due to NiO and GDC10 in FTIR spectrum of nano-composite confirms formation of nano-composite. Also for the nano-composites with 30–60 mol % NiO showed a porous microstructure composed of uniformly distributed and well-connected constituent grains. The activation energy calculated from the d.c. conductivity decrease with addition of NiO and shows *S* type behavior with increase in conductivity for 40 mol % NiO indicating percolation limit.

Acknowledgements

The authors are very much thankful to Board of Research in Nuclear Sciences (BRNS) for financial assistance. Also the authors are thankful to UGC-DAE Consortium for Scientific Research, Indore, for providing characterization facility.

References

[1] C.C. Liang, A.V. Joshi, N.E. Hamilton, Solid-state storage batteries, Journal of Applied Electrochemistry 8 (1978) 445–454.
[2] A. Menne, W. Wepppner, Redox reaction mechanisms at the AgCl/chlorine gas interface, Electrochimica Acta 1823 (1991) 11–12.
[3] Z. Wu, M. Liu, Modelling of ambipolar transport properties of composite mixed ionic-electronic conductors, Solid State Ionics 93 (1997) 65–84.
[4] N.Q. Minh, Ceramic fuel cells, Journal of the American Ceramic Society 76 (1993) 563–588.
[5] T.E. Mady, J.T. Yates, D.R. Scndstrom Jr., R.J.H. Voorhoeve, in: N.B. Hannay (Ed.), Treatise on Solid state Chemistry, vol. 6B, Plenum Press, New York, 1976, p. 1.
[6] Changsheng Ding, Hongfei Lin, Kazuhisa Sato, Toshiyuki Hashida, Synthesis of NiO–$Ce_{0.9}Gd_{0.1}O_{1.95}$ nanocomposite powders for low-temperature solid oxide fuel cell anodes by co-precipitation, Scripta Materialia 60 (2009) 254–256.
[7] Q. Jeangros, A. Faes, J.B. Wagner, T.W. Hansen, U. Aschauer, J. Vanherle, A. Hessler-Wyser, R.E. Dunin-Borkowski, In situ redox cycle of a nickel–YSZ fuel cell anode in an environmental transmission electron microscope, Acta Materialia 58 (2010) 4578–4589.
[8] S.P. Jiang, Sam Zhang, Y.D. Zhen, A.P. Koh, Performance of GDC-impregnated Ni anodes of SOFCs, Electrochemical and Solid-State Letters 7 (9) (2004) A282–A285.
[9] Changjing Fu, Siew Hwa Chan, Qinglin Liu, Xiaoming Ge, G. Pasciak, Fabrication and evaluation of Ni–GDC composite anode prepared by aqueous based tape casting method for low-temperature solid oxide fuel cell, International Journal of Hydrogen Energy 35 (2010) 301–307.
[10] L.D. Jadhav, M.G. Chourashiya, K.M. Subhedar, A.K. Tyagi, J.Y. Patil, Synthesis of nanocrystalline Gd doped ceria by combustion technique, Journal of Alloys and Compounds 470 (2009) 383–386.
[11] Chanrong Xia, Meilin Liu, Microstructures, conductivities, and electrochemical properties of $Ce_{0.9}Gd_{0.1}O_2$ and GDC–Ni anodes for low-temperature SOFCs, Solid State Ionics 152–153 (2002) 423–430.
[12] J. Christopher, M.P. Sridhar Kumar, C.S. Swamy, Thermal studies on high temperature oxidation behaviour of nickel containing Ab, type intermetallics, Thermochimica Acta 161 (1990) 207–215.
[13] R.V. Wandekar, M. Ali (Basu), B.N. Wani, S.R. Bharadwaj, Physicochemical studies of NiO–GDC composites, Materials Chemistry and Physics 99 (2006) 289–294.
[14] Martin, J. Buerger, Crystal Structure Analysis, John Wiley and Sons, New York, 1960.
[15] E. Ramachandran, K. Baskaran, S. Natarajan, XRD, thermal, and FTIR and SEM studies on gel grown γ-glycine crystals, Crystal Research and Technology 42 (2007) 73–77.
[16] Chunhui Shen, L.L. Shaw, FTIR analysis of the hydrolysis rate in the sol–gel formation of gadolinia-doped ceria with acetylacetonate precursors, Journal of Sol–Gel Science and Technology 53 (2010) 571–577.
[17] Tao Wang, Du-Cheng Sun, Preparation and characterization of nanometer-scale powders ceria by electrochemical deposition method, Materials Research Bulletin 43 (2008) 1754–1760.
[18] Young Min Park, Gyeong Man Choi, Microstructure and electrical properties of YSZ–NiO composites, Solid State Ionics 120 (1999) 265–274.
[19] H.A. Taroco, J.A.F. Santos, R.Z. Domingues, T. Matencio, Ceramic materials for solid oxide fuel cells, advances in ceramics – synthesis and characterization, Processing and Specific Applications (2011) 423–446.
[20] U.P. Muecke, Silvio Graf, Urs Rhyner, L.J. Gauckler, Microstructure and electrical conductivity of nanocrystalline nickel and nickel oxide/gadolinia-doped ceria thin films, Acta Materialia 56 (2008) 677–687.